

# Three Exit Channels in the Fission of $^{235}\text{U}(\text{n}, \text{f})$

H.-H. Knitter, F.-J. Hambsch, and C. Budtz-Jørgensen

Commission of the European Communities, Joint Research Centre,  
Central Bureau for Nuclear Measurements, Geel, Belgium

J. P. Theobald

Institut für Kernphysik, Technische Hochschule, Darmstadt, Germany

Z. Naturforsch. **42a**, 786–790 (1987); received May 28, 1987

A formula for the fission fragment yield area in the coordinate system of the fragment total kinetic energy and of the fragment mass is presented. It was deduced along the lines of the multi-exit-channel model of fission elaborated by Brosa, Grossmann and Müller. This formula was fitted to the fragment mass-, average total kinetic energy-, and variance distributions of the thermal neutron induced fission of  $^{235}\text{U}$ . The obtained parameters are compared with the theoretical predictions. Further improvements of the fragment yield representation are discussed.

## 1. Introduction

The dip of about 22 MeV in the average total fragment kinetic energy in the symmetric mass region of the thermal neutron induced fission of  $^{235}\text{U}$  is a longstanding experimental fact which remained unexplained by previous fission models. Also the calculations of variances of the fragment total kinetic energy and mass distributions within the framework of previous theories and fission models do not give a satisfactory description of the experimentally observed variances [1]. Two-mode-fission was already postulated as early as 1951 by Turkevich and Niday [2] on an empirical base and was applied by Britt et al. [3] to the fission of light actinides. Also recently this model was used by Itkis et al. [4] and Hulet et al. [5] in the pre-actinide and very heavy actinide regions, respectively. However, this picture was not successful for medium weight actinides and fails therefore as a general model for fission throughout the whole mass range.

Recently Brosa, Grossmann and Müller [6–11] performed Strutinski-type calculations for several nuclei covering the mass range from  $^{227}\text{Ac}$  to  $^{258}\text{Fm}$ , where the potential energy of the compound system was obtained also for large deformations up to the scission point. These calculations indicate the

presence of several fission paths or channels, whose accessibilities are different for different fissioning nuclei. They predict the existence of four and of three fission exit channels for  $^{252}\text{Cf}(\text{sf})$  [6] and  $^{235}\text{U}(\text{n}, \text{f})$  [7], respectively. Therefore we analysed our measurements of the mass-, kinetic energy-, and variance distributions along the lines of this model.

## 2. Fragment Yield as Function of Mass and Total Kinetic Energy

According to Brosa, Grossmann and Müller [6–11] each exit channel has its own characteristic shape at the scission point. For  $^{236}\text{U}$  they find a super-long symmetric channel and two asymmetric channels, standard I and standard II, which have a symmetric and two asymmetric scission shapes, respectively [7]. These three scission shapes have different semi-lengths  $l_h$  and neck positions  $z_n$  with respect to the center. The average fragment mass for each fission channel is deduced from the position of the neck  $z_n$ . The width of the mass distribution for each channel is obtained from the frequency distribution of the random neck rupture positions [9].

For the symmetric superlong channel, the average mass is 118 and the mass distribution must be symmetric around this mass. For the two predicted asymmetric fission channels mass distribution with small asymmetries are possible. However, in the present work, we assume the mass distributions of

Reprint requests to Dr. J. P. Theobald, Institut für Kernphysik, Technische Hochschule Darmstadt, D-6100 Darmstadt.

0932-0784 / 87 / 0800-0786 \$ 01.30/0. – Please order a reprint rather than making your own copy.



Dieses Werk wurde im Jahr 2013 vom Verlag Zeitschrift für Naturforschung in Zusammenarbeit mit der Max-Planck-Gesellschaft zur Förderung der Wissenschaften e.V. digitalisiert und unter folgender Lizenz veröffentlicht: Creative Commons Namensnennung-Keine Bearbeitung 3.0 Deutschland Lizenz.

Zum 01.01.2015 ist eine Anpassung der Lizenzbedingungen (Entfall der Creative Commons Lizenzbedingung „Keine Bearbeitung“) beabsichtigt, um eine Nachnutzung auch im Rahmen zukünftiger wissenschaftlicher Nutzungsformen zu ermöglichen.

This work has been digitalized and published in 2013 by Verlag Zeitschrift für Naturforschung in cooperation with the Max Planck Society for the Advancement of Science under a Creative Commons Attribution-NoDerivs 3.0 Germany License.

On 01.01.2015 it is planned to change the License Conditions (the removal of the Creative Commons License condition “no derivative works”). This is to allow reuse in the area of future scientific usage.

all channels to be symmetric and of Gaussian shape:

$$Y(M) = \sum_{i=1}^3 \frac{W_i}{\sqrt{2\pi} \sigma_{M_i}} \cdot \exp \left\{ -\frac{(M - M_i)^2}{2\sigma_{M_i}^2} \right\}. \quad (1)$$

The index  $i$  indicates the fission channel,  $W_i$  the relative population of the channel,  $M_i$  the average fragment mass of the heavy fragment and  $\sigma_{M_i}$  the width of the mass distribution for channel  $i$ . This representation was used already by Straede, Budtz-Jørgensen, and Knitter for the description of the mass distributions of  $^{235}\text{U}$  (n, f) measured at different incident neutron energies [12], [16]. Eq. (1) was used to fit the pre-neutron emission mass distribution for the thermal neutron induced fission of  $^{235}\text{U}$  determined by Hambsch [13]. The experiment will be described elsewhere [13]. The full thick line through the experimental points of the mass distribution in the upper part of Fig. 1 represents the result of the fit and is a superposition of the three fission channels. The three thin lines give the mass distributions for the superlong, the standard I and the standard II fission channels separately. For the mass region below about mass 140 a superposition of the fission channels is observed, whereas above that mass there is only the contribution from the standard II channel. The numerical values of the parameters and their errors are given in Table 1.

Since the fragment yield was measured not only as function of the mass split but also as function of the sum of both fragment kinetic energies, the aim was to find a representation of the yield as function of both,  $Y(M, \text{TKE})$ , where TKE is the kinetic energy of both fragments. With the assumption of zero pre-scission kinetic energy the total kinetic energy is equal to the Coulomb repulsion energy. With the further assumption of an unchanged charge distribution in the nuclear charge division to the fragments, the Coulomb energy of each fission channel is given by

$$\text{TKE} = \frac{\frac{M}{A} \cdot Z \left( Z - \frac{M}{A} \cdot Z \right) \cdot e^2}{D_i} = \frac{F(M)}{D_i}, \quad (2)$$

where  $A$  and  $Z$  are the nuclear mass and charge of the fissioning compound nucleus and  $e$  is the elementary charge.  $D_i$  is the average charge distance between the charge centers of the nascent fragments. According to the Brosa-Grossmann-Müller model

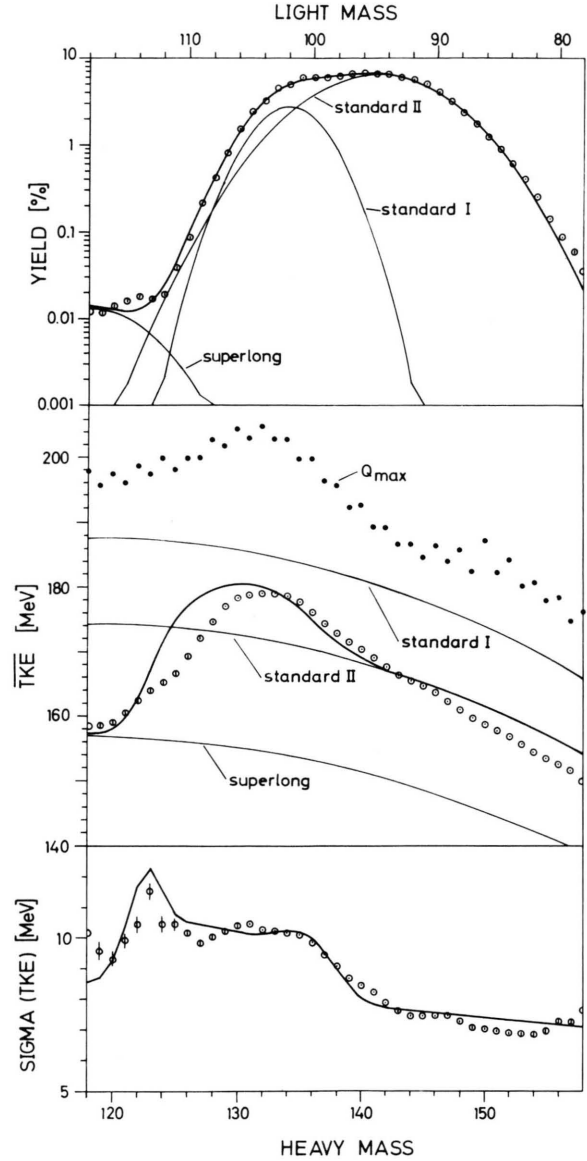


Fig. 1. The fission fragment yield from  $^{235}\text{U}$  (n, f) at thermal energy, the  $Q_{\max}$ -value, the average total kinetic energy and sigma (TKE) are plotted versus the heavy and light fragment mass [13]. The thick lines through the experimental points are the results of fits. The thinner lines represent the yield and the average total kinetic energy of the partial fission exit channels.

this average distance is assumed to be a constant for each fission channel  $i$ . When the compound nucleus deforms towards the scission shape it moves along the fission valley of the potential energy surface through one of the exit channels [6]. The frequency dis-

Table 1. The upper part represents the parameters obtained from the fit to the experiments [13]. The lower data are from theory [15].

Channel name	Experiment [13]					
	$W_i$ [%]	$M_i$ [u]	$\sigma_{M_i}^2$ [u <sup>2</sup> ]	$D_i$ [fm]	$\sigma_{D_i}$ [fm]	TKE <sub><i>i</i></sub> [MeV]
Superlong	$0.069 \pm 0.010$	118	$17.1 \pm 6$	$19.4 \pm 0.9$	$1.00 \pm 0.68$	$157 \pm 7$
Standard I	$18.3 \pm 0.3$	$133.9 \pm 0.1$	$6.9 \pm 0.4$	$16.0 \pm 0.1$	$0.800 \pm 0.001$	$187 \pm 1$
Standard II	$81.4 \pm 0.4$	$141.1 \pm 0.1$	$24.6 \pm 0.4$	$17.5 \pm 0.1$	$0.691 \pm 0.005$	$167 \pm 1$
	Theory [15]					
		$M_i$ [u]	$\sigma_{M_i}^2$ [u <sup>2</sup> ]	$l_h/S'$ [fm]		TKE <sub><i>i</i></sub> [MeV]
Superlong	–	$118 \pm 5$	$30 \pm 15$	$19.2 \pm 0.5$	–	$159 \pm 4$
Standard I	–	$133 \pm 5$	$4.3 \pm 2.1$	$16.4 \pm 0.5$	–	$183 \pm 6$
Standard II	–	$147 \pm 5$	$35 \pm 17$	$19.0 \pm 0.5$	–	$151 \pm 4$

tribution of the rupture length  $D$  will depend on the details of the potential energy landscape in the neighbourhood of the average charge distance  $D_i$ . Since such details are not yet known from theory, Gaussian frequency distributions are assumed:

$$H_i(D, M) = \frac{1}{\sqrt{2\pi} \sigma_{D_i}} \cdot \exp\left(-\frac{(D - D_i)^2}{2\sigma_{D_i}^2}\right). \quad (3)$$

$\sigma_{D_i}$  is the variance of the charge distance at scission. This frequency distribution can only be an approximation because it does not contain the Rayleigh instability criterion [10, 14], which allows a rupture only if the ratio of the compound system semi-length  $l_h$  to the neck radius  $r_n$  exceeds a certain value. The compound system must exceed a certain minimum length, according to this criterion, before scission can take place, and therefore the total kinetic energy is limited to a finite maximum value. This is not the case in the ansatz made in (3). A combination of (1), (2) and (3) gives the yield distribution as function of mass and total kinetic energy,

$$Y(M, \text{TKE}) = \sum_{i=1}^3 \frac{W_i}{\sqrt{2\pi} \sigma_{M_i}} \cdot \exp\left(-\frac{(M - M_i)^2}{2\sigma_{M_i}^2}\right) \cdot \frac{F(M)}{C_i \sqrt{2\pi} \sigma_{D_i} \text{TKE}^2} \cdot \exp\left(-\frac{\left(\frac{F(M)}{\text{TKE}} - D_i\right)^2}{2\sigma_{D_i}^2}\right) \quad (4)$$

with the normalization

$$C_i = \int_0^\infty \frac{F(M)}{\sqrt{2\pi} \sigma_{D_i} \cdot \text{TKE}^2} \cdot \exp\left(-\frac{\left(\frac{F(M)}{\text{TKE}} - D_i\right)^2}{2\sigma_{D_i}^2}\right) \cdot d \text{TKE}. \quad (5)$$

This description of the fission fragment yield as function of mass and total kinetic energy was used to fit simultaneously the average total kinetic energy TKE and its variance as function of mass. The parameters  $W_i$ ,  $M_i$  and  $\sigma_{M_i}$  were kept fixed at the values obtained from the fit with (1) to the mass distribution alone. The six parameters  $D_i$  and  $\sigma_{D_i}$  obtained by the fit are given in Table 1. The two thick lines in the middle and lower part of Fig. 1 show the results of the fit in comparison to the experimental TKE and to sigma (TKE), respectively.

### 3. Discussion

The gross structure of the mass distribution of the thermal neutron induced fission of  $^{235}\text{U}$  is well described by the sum of the three Gaussian functions which can now be interpreted as individual contributions of the three fission channels as proposed in the Brosa-Grossmann-Müller model [7]. The fit curve through the experimental average total kinetic energies deviates nowhere by more than 5% from the experiment. However, from the

physics point of view it is more important that the shape of the curve and the large drop for symmetric fission are understood in the frame of the above model. The curve for the sigma of TKE shows evidently the presence of three channels. Above mass 142 the variance decreases only very slowly with increasing mass. This is due to the mass dependence in the term for the energy distribution of (4) and (5). Then, towards lower mass numbers there is a broad region of overlap of the standard I and standard II channels with comparable intensities, which leads to an increase of the variance. The largest value of sigma at mass 123 is due to the superposition of the superlong and standard II channels, which have nearly the same intensity at this mass as can be seen from Figure 1.

In Table I the numerical values for the parameters of (4) and the average total kinetic energy for each channel, as obtained from the experiment, are given together with the parameter values obtained from theory [15]. The parameters obtained from theory [15] are presented in Table I in the corresponding columns below the experimental ones. The value from theory to be compared with the present average charge distance at scission is  $l_h/S'$ , where  $S'$  contains the correction for the shape of the nascent fragments to the Coulomb repulsion energy and for the nuclear interaction between them [9]. Good agreement within the errors is obtained between theory and experiment for all the parameters. Only the charge distance of the standard II channel is slightly off by 1.5 fm and associated with it the TKE for this channel.

Although the present parametrization of the Brosa-Grossmann-Müller model describes the above mentioned quantities well, it fails to describe the third moments of the total kinetic energy distributions, where a negative coefficient of disymmetry between  $-0.35$  and  $-0.15$  was measured in the mass region from 125 to 160. In the mass region above 142 only the standard II channel is open, and this channel alone shows already a small asymmetry of the total kinetic energy distributions. Therefore an improved frequency distribution for  $D$  should be slightly asymmetric and contain the Rayleigh instability criterion, which limits the yield in the high energy wings of the energy distributions at a finite maximum energy value.

The fission fragment mass-, total kinetic energy-, and variance distributions were recently measured

as function of incident neutron energy by Straede, Budtz-Jørgensen, and Knitter [12]. They fitted the mass distributions with two Gaussian functions in the asymmetric mass peak and with one in the symmetric mass region. These Gaussians are now interpreted as representations of the yields from the three fission exit channels predicted by the Brosa-Grossmann-Müller model for  $^{235}\text{U}$  (n, f). The experiment showed no significant change of the mass distribution below 2 MeV incident neutron energy, however a small increase of the total kinetic energy for all fragments. Above 2 MeV incident neutron energy a decrease in the population of the standard I channel and an increase in the population of the two other channels were observed. The drop of the total kinetic energy averaged over all fragments with incident neutron energy measured in that experiment can be explained in the frame of the above model by the change of the populations in the three fission channels. It is clearly seen in Fig. 8 of [12] that the average total kinetic energy for mass splits around mass 134 drops with increasing incident neutron energy compared to the thermal value. This is due to a smaller contribution from the standard I channel, which fissions with higher total kinetic energy than the other fission channels. Therefore a net reduction of the total kinetic energy averaged over all fragments is observed.

#### 4. Conclusions

The present representation of the fission fragment yield area as function of the sum of both fragment kinetic energies and of the fragment mass describes for the thermal neutron induced fission of  $^{235}\text{U}$  the mass yield, the average total kinetic energy, and the variance with model parameters in sound agreement with those predicted by Brosa, Grossmann and Müller. With this model one can now explain quantitatively the gross structure of these distributions. Further work is required on details of the potential energy landscape near the scission point in order to obtain a frequency distribution for  $D$ , (3), from theory. Such a distribution must then be improved to describe the third moment of TKE and the low yield region close to the  $Q$ -value. The present formulation for the yield should be applied also to other fissioning systems to see whether the model succeeds also there.

We thank very much U. Brosa, S. Grossmann, and A. Müller for several very helpful discussions about their theoretical model. We thank U. Brosa

for the communication of results contained in Table I prior to publication.

- [1] Yu. A. Lazarev, Proc. of the EPS Topical Conf. on Large Amplitude Collective Nuclear Motions, Keszthely, Hungary, 10–16 June 1979, Vol. I, p. 244.
- [2] A. Turkevich and J. B. Niday, Phys. Rev. **84**, 52 (1951).
- [3] H. C. Britt, H. E. Wegner, and J. C. Gursky, Phys. Rev. **129**, 2239 (1963).
- [4] M. G. Itkis, V. N. Okolovich, A. Ya. Rusanov, and G. N. Smirenkin, Z. Phys. **A 320**, 433 (1985).
- [5] E. K. Hulet, J. F. Wild, R. J. Dougan, R. W. Loughheed, J. H. Landrum, A. D. Dougan, M. Schädel, R. L. Hahn, P. A. Baisden, C. M. Henderson, R. J. Dupzyk, K. Sümmerner, and G. R. Bethune, Phys. Rev. Lett. **56**, 313 (1986).
- [6] U. Brosa, S. Grossmann, and A. Müller, Z. Naturforsch. **41a**, 1341 (1986).
- [7] U. Brosa, S. Grossmann, and A. Müller, Proc. of XVI<sup>th</sup> Intern. Symposium on Nuclear Physics, Gaussig, Dresden, GDR, Nov. 1986.
- [8] U. Brosa, S. Grossmann, and A. Müller, Phys. Rev. **C 32**, 1438 (1985).
- [9] U. Brosa and S. Grossmann, Z. Phys. **A 310**, 177 (1985).
- [10] U. Brosa and S. Grossmann, J. Phys. **G 10**, 933 (1984).
- [11] U. Brosa, S. Grossmann, and A. Müller, Z. Phys. **A 325**, 241 (1986).
- [12] Ch. Straede, C. Budtz-Jørgensen, and H.-H. Knitter, Nucl. Phys. **A 462**, 85 (1987).
- [13] F.-J. Hambsch, Ph.D. Thesis, Technische Hochschule Darmstadt, Germany, and Commission of the European Communities J.R.C., Central Bureau for Nuclear Measurements, Geel, Belgium 1987.
- [14] F. R. S. Lord Rayleigh, Proc. London Math. Soc. **X**, 4 (1878).
- [15] U. Brosa, private communication, March 1987.
- [16] Ch. Straede, Neutron Induced Fission of  $^{235}\text{U}$ , Ph.D. Thesis, University of Aarhus, Denmark, and Commission of the European Communities, J.R.C., Central Bureau for Nuclear Measurements, Geel, Belgium (May 1985).